Surface & Coatings Technology 320 (2017) 614–618

Contents lists available at ScienceDirect

Surface & Coatings Technology

journal homepage: www.elsevier.com/locate/surfcoat

Tin repellence on wave-soldering stainless steel holders coated with Ti/TiC/DLC

Shu Xiao [a], Zhongzhen Wu [a,*], Liangliang Liu [a], Ricky K Y Fu [c], Wan Li [c], Xiubo Tian [a,b], Paul K Chu [c], Feng Pan [a]

[a] School of Advanced Materials, Peking University Shenzhen Graduate School, Shenzhen 518055, China
[b] State Key Laboratory of Advanced Welding and Joining, Harbin Institute of Technology, Harbin 150001, China
[c] Department of Physics and Materials Science, City University of Hong Kong, Tat Chee Avenue, Kowloon, Hong Kong, China

ARTICLE INFO

Article history:
Received 4 August 2016
Revised 19 October 2016
Accepted in revised form 22 October 2016
Available online 23 October 2016

Keywords:
Ti/TiC/DLC coatings
Tin repellence
Lead-free soldering
Stainless steel

ABSTRACT

Lead-free solder is widely used in the industry, especially in wave soldering. However, the stainless steel holders used in wave soldering are prone to corrosion by the lead-free solder due to increased reactive wetting. Besides, owing to the high affinity between the holders and solder, they are often used to take solder out of the container. To improve tin repellence and the mechanical properties of the stainless steel holders, Ti/TiC and Ti/TiC/DLC coatings are deposited by filtered cathodic vacuum arc (FCVA) and plasma immersion ion implantation and deposition (PIII&D). The morphology, structure, composition, microhardness, wear resistance, electrochemical properties, and wetting characteristics are investigated systematically. The DLC coating, which has an amorphous structure and I_D/I_G ratio of about 0.55, further enhances the frictional properties, corrosion resistance, and hydrophobic characteristics of the Ti/TiC structure. The surface-modified holders show excellent tin repellence in wave soldering.

1. Introduction

Lead-free solder has replaced Pb-based solder in the electrical industry [1–3], especially in wave soldering. However, the stainless steel holders used in wave soldering are corroded by the lead-free solder due to enhanced reactive wetting. Moreover, owing to the good affinity between the holders and solder, the latter is often taken out of the container by the holders for use on printed circuit boards (PCB) thus exacerbating the corrosion problem and solder wastage [4–6]. Alternative materials such as Ti, Ti alloys, and cast iron which have better corrosion resistance and tin repellence have been proposed to replace stainless steel to expand the service life and reduce wastage of lead-free solder. However, Ti is more expensive than stainless steel and the poor formability of cast iron makes wave soldering of components with a complex shape difficult [7]. Hence, there has been increasing interest in modifying the surface of stainless steel holders in lieu of replacing them. For example, PPS and nylon 66 organic coatings with smaller surface energies show good wetting resistance but the mechanical performance and thermal stability of organic coatings are generally poor [8,9]. In comparison, ceramic coatings such as Cr_xC_y and Ti/TiC are more robust while offering good mechanical and corrosion performance. In spite of the slightly worse wetting performance, Ti/TiC coatings have been shown to have some advantages in wave soldering [10].

In this work, in order to enhance tin repellence and wear resistance, a diamond-like carbon (DLC) layer with an optimal thickness is deposited on the Ti/TiC structure. Considering the stress and adhesion issues between the DLC coating and substrate [11,12], energetic plasma immersion ion implantation and deposition (PIII&D) is employed [13,14]. PIII&D is a non-line-of-sight technique suitable for samples with complex geometry [15]. The morphology, structure, composition, microhardness, wear resistance, electrochemical properties, and wetting characteristics of the coated materials are determined in details and our results reveal that the surface treatment improves the mechanical properties and tin repellence of stainless steel holders.

2. Experimental details

The experiments were carried out in a chamber with a diameter of 100 cm and height of 80 cm. The vacuum chamber was evacuated to a base pressure of 1×10^{-3} Pa prior to sample loading. The silicon (100) and stainless steel substrates were ultrasonically cleaned in ethanol, acetone, and deionized water for 20 min each. After the samples were cleaned by bombarding with 1 KeV argon ions for 20 min in the vacuum chamber, Ti and TiC intermediate layers were deposited without external heating by FCVA using a Ti target (99.9 at.%) in the presence of a carrier gas (Ar, 99.999% pure) and reactive gas (C_2H_2, 99.8% pure).

* Corresponding author.
E-mail address: wuzz@pkusz.edu.cn (Z. Wu).

http://dx.doi.org/10.1016/j.surfcoat.2016.10.059
0257-8972/

The distance between the Ti target and substrate was 10 cm. The current was 60 A and the voltage was 45 V. The temperature was about 150 °C during deposition because heating by the arc, although no extra heating was applied. The thickness of the Ti and TiC layers was about 100 nm and 1 μm, respectively. The C_2H_2 partial pressure was 0.5 Pa and bias was −200 V. The DLC layer was deposited using an anode layer source at a power of 90 W, pressure of 0.3 Pa, 10 sccm Ar, and 30 sccm C_2H_2. Negative high-voltage pulses (9.5 kV, 50 μs, 50 Hz) were applied to the substrate to conduct PIII&D. To obtain different DLC thicknesses, the deposition time was 30 min, 60 min, 90 min and 120 min. After PIII&D, the samples were cooled naturally in the chamber under vacuum.

The crystalline structure of the coatings was determined by X-ray diffraction (Bruker D8 Advance) in the continuous scanning mode using Cu K_α radiation ($\lambda = 0.154056$ nm) at room temperature (RT) and the 2θ range is from 10° to 80° with a 0.1° step size. The I_D/I_G ratio was determined at room temperature on a high-resolution confocal Raman microscope (Horiba Jobin-YvonLabRam HR VIS) equipped with a 532 nm laser as the excitation source. The surface morphology was examined by field-emission scanning electron microscopy (FE-SEM, ZEISS SUPRA® 55). A microhardness tester (HVS-1000) was employed to determine the microhardness of the coatings using a load of 20 g for 10 s and 20 measurements were made to obtain the average. A ball-on-disk tester was used to evaluate the wear resistance under ambient conditions (relative humidity of 25 ± 1 RH% and temperature of 20 ± 1 °C). A Φ6.636 mm SiC ball was used against the coating at 100 N and 80 rpm with a wear radius of 3 mm. The electro-chemical corrosion test was performed on a Reference 600 Electrochemical Analyzer. The solution was 3.0 wt.% NaCl and polarization was performed at a scanning rate of 3 mV/s. An optical contact angle instrument (Precise Test Equipment Co., Ltd.) was used to observe the solder droplet, a homemade heating unit was assembled on the stage to melt the solder during the test. It was used to melt the solder into a droplet and the temperature here was about 280 °C.

3. Results and discussion

The XRD patterns of the Ti/TiC/DLC coatings deposited on the stainless steel samples with different DLC layer thicknesses are depicted in Fig. 1. Besides peaks from the substrate, only Ti and TiC peaks can be observed. The Ti peaks, which may be attributed to the transition layer and unreacted Ti, show the Ti (100), Ti (101), and Ti (103) preferred orientations with 2θ values of 35.04°, 40.10°, 74.27°, respectively. The TiC diffraction peaks, TiC (111) and TiC (220) at 36.57° and 59.11°, respectively, can be observed by XRD but no DLC peaks can be observed suggesting an amorphous structure [16,17].

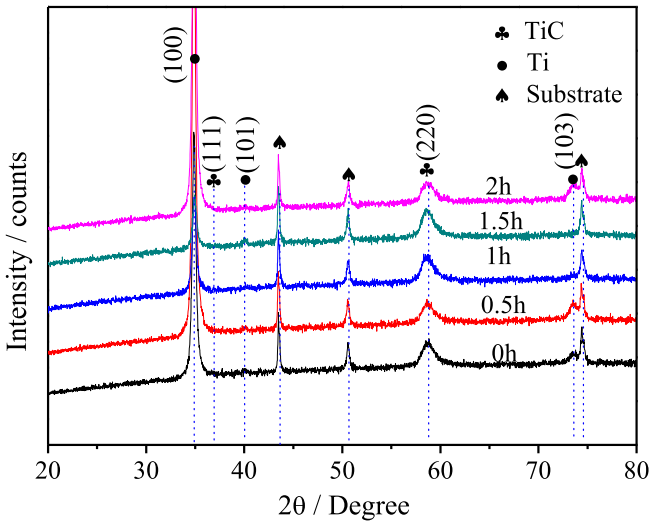

Fig. 1. XRD patterns of the Ti/TiC/DLC coatings with different DLC thicknesses.

The microstructure of the Ti/TiC/DLC coatings is investigated by Raman scattering. The spectrum can be deconvoluted into the disorder D peak and G peak. According to the Tunistra-Koenig relationship for amorphous carbon [18,19], the intensity ratios of the two fitted Gaussian peaks, I_D/I_G, is proportional to the cluster diameter and a small I_D/I_G usually means a large content of sp^3 bonding in the DLC. The Raman results are summarized in Table 1. The I_D/I_G ratio increases slightly with DLC film thickness and the largest value is 0.59 corresponding to the largest DLC thickness of 400 nm. Hence, a long deposition time decreases the fraction of sp^3 in the DLC coatings [20].

The cross-sectional SEM images of the Ti/TiC/DLC coatings are presented in Fig. 2 and the Ti/TiC and DLC layers can be identified clearly. The Ti/TiC interlayer which is crucial to good adhesion between the DLC layer and substrate has the typical columnar and dense structure [21,22]. Since the Ti/TiC layer is prepared by FCVA, there are some macropaticles and defects on the surface. However, DLC can fill the space between the macroparticles thus eliminating the defects and decreasing the surface roughness of the coating. With increasing deposition time, the DLC thickness increases and surface roughness decreases. When the deposition time is 2.0 h, the DLC thickness is 400 nm.

The microhardness of the Ti/TiC/DLC coatings is shown in Fig. 3. The microhardness was obtained on a Vickers microhardness tester. Although the microhardness includes contributions from the substrate making them smaller than the actual value [23,24], it also shows the enhancement effect to the substrate which is our main concern. All the coatings are harder than the substrate and the microhardness increases if the DLC layer is thicker. The largest microhardness is 1013 HV observed from the thickest DLC layer. The fluctuation in the microhardness decreases with DLC thickness possibly because DLC fills the space between the macroparticles and defects.

The tribological behavior of the stainless steel substrate, Ti/TiC coating, and Ti/TiC/DLC coating with a 400 nm thick DLC is shown in Fig. 4(a). An obvious decrease in the friction coefficient is observed from the Ti/TiC and Ti/TiC/DLC coatings compared to the stainless steel substrate. The friction coefficient decreases from 0.12 to 0.08 on the 400 nm DLC layer indicative of self-lubricating effects [25,26]. The tracks on the Ti/TiC coating and the Ti/TiC/DLC coating are shown in the Fig. 4(b) and Fig. 4(c), respectively. The one on the Ti/TiC coating is deeper and wider than that on the Ti/TiC/DLC coating, indicating that the Ti/TiC/DLC coating has better tribological properties as a result of the higher microhardness and smoother surface.

The polarization curves of the stainless steel substrate, Ti/TiC, and Ti/TiC/DLC (2.0 h) samples are displayed in Fig. 5. The Ti/TiC and Ti/TiC/DLC coatings exhibit larger corrosion potentials, smaller corrosion currents, and better corrosion resistance than the substrate. The corrosion potentials of the Ti/TiC sample increase

Table 1
Raman scattering results of the Ti/TiC/DLC coatings.

Samples	D band position (cm^{-1})	FWHM D (cm^{-1})	G band position (cm^{-1})	FWHM G (cm^{-1})	I_D/I_G
1	1336.2	356.2	1528.4	183.4	0.54
2	1337.1	356.3	1528.0	183.3	0.56
3	1340.8	354.35	1528.9	182.48	0.57
4	1338.4	358.3	1529.7	177.5	0.59

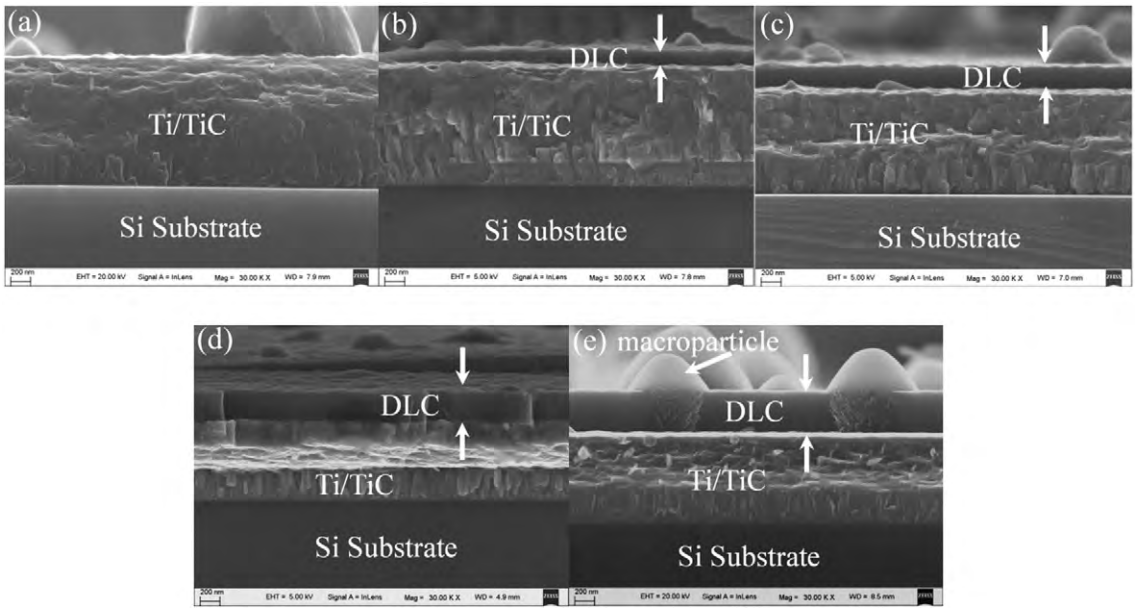

Fig. 2. Cross-sectional SEM images of the Ti/TiC/DLC coatings deposited on silicon for different deposition time: (a) 0 h, (b) 0.5 h, (c) 1.0 h, (d) 1.5 h, and (e) 2.0 h.

from −0.671 V to −0.288 V and the corrosion currents decrease from 51 μA to 1.84 μA. After deposition of the 400 nm DLC layer, the corrosion potential increases to −0.280 V and corrosion current diminishes to 0.61 μA. Some corrosion channels in the coating and defects on the surface can be found from the Ti/TiC coating [10]. In comparison, the DLC layer has a dense amorphous structure blocking the corrosion channels giving rise to better corrosion resistance [22, 27].

The contact angles of liquid lead-free solder on the Ti/TiC/DLC samples determined by the modified sessile drop method are shown in Fig. 6. Compared to the average contact angle on the stainless steel sample (126.7°), both Ti/TiC and Ti/TiC/DLC show deteriorated wetting behavior. The average contact angles on Ti/TiC and Ti/TiC/DLC are 134.6°, 137.3°, 137.4°, 139.2° and 141.2°, respectively. With increasing DLC thickness, the contact angles increase continuously and it may be attributed to the decreased height of macropaticles on the surface as DLC fills the gaps. The better hydrophobicity of Ti/TiC/DLC towards lead-free solder may stem from the synergistic effects of the amorphous DLC structure [28], less defects, and smoother surface.

The repellence performance of the stainless steel holders with and without the coatings in wave soldering is shown in Fig. 7 (a). A mass of solder usually adheres on the bare stainless steel holders as it is taken from the container. On the coated holder, the quantity of the adhered solder decreases and the Ti/TiC/DLC sample shows the best tin repellence compared to TiN and TiC as shown in Fig. 7 (b).

4. Conclusion

Ti/TiC/DLC coatings are deposited on stainless steel holders by FCVA and PIII&D to improve the corrosion resistance and Sn repellence in

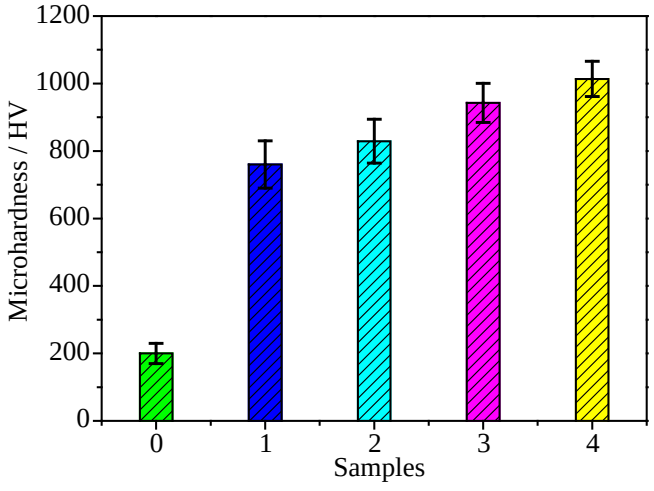

Fig. 3. Microhardness of the Ti/TiC/DLC coatings produced with different deposition time of DLC layers.

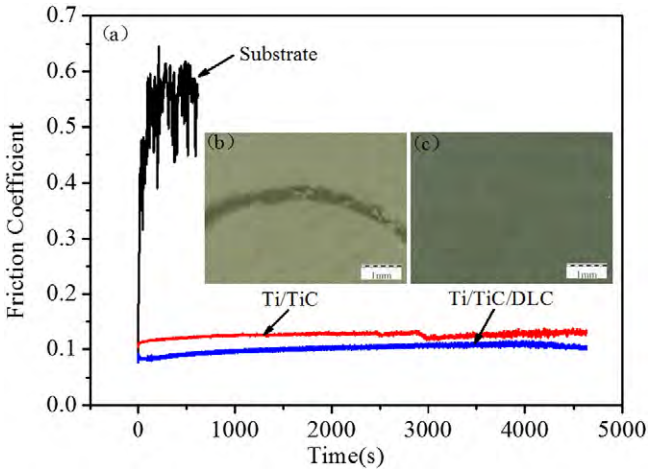

Fig. 4. (a) Friction coefficients of the stainless steel, Ti/TiC, and Ti/TiC/DLC samples; (b) wear track on the Ti/TiC coating; (c) Wear track on the Ti/TiC/DLC coating.

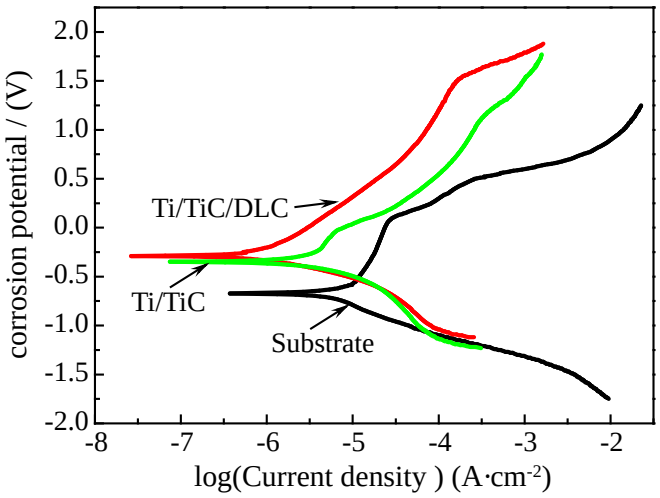

Fig. 5. Polarization curves of the different samples.

liquid lead-free solder. The structure, morphology, and mechanical properties of the Ti/TiC/DLC coatings are experimentally investigated for different DLC deposition time. As the deposition time is increased, the I_D/I_G ratio increases slightly indicating a reduced sp^3 fraction. Because the DLC fills the space between the macroparticles and defects, the highest microhardness of 1013 HV is achieved on the sample with the thickest DLC layer of about 400 nm. The DLC layer with a dense amorphous structure impedes corrosion and shows better corrosion resistance. Compared to the pristine substrate and Ti/TiC coating, the Ti/TiC/DLC coating has better tribological properties as a result of the higher microhardness and lower roughness. The better hydrophobicity of Ti/TiC/DLC to lead-free solder may stem from the synergistic effects of the amorphous DLC structure, reduced defects, as well as smoother surface. When the holders are coated, the quantity of the adhered solder decreases and the Ti/TiC/DLC shows the best tin repellence. The Ti/TiC/DLC coating can protect the stainless steel holders and have great potential in wave soldering involving lead-free solder.

Acknowledgements

This work was financially supported by Natural Science Foundation of China (No. 51301004, U1330110), Shenzhen Science and Technology Research Grants (JCYJ20140903102215536 and JCYJ20150828093127698), and City University of Hong Kong Applied Research Grant (ARG) No. 9667122.

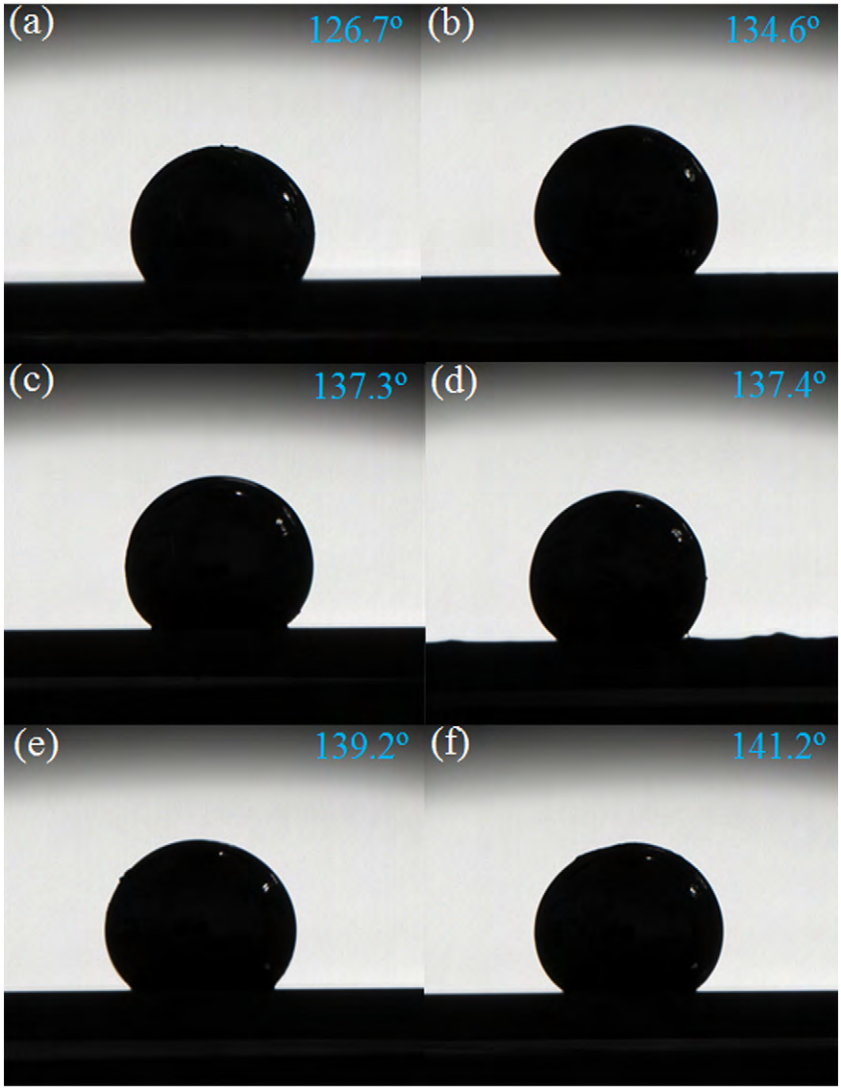

Fig. 6. Contact angles of the liquid lead-free solder droplet on (a) stainless steel, (b) Ti/TiC, (c) Ti/TiC/DLC 0.5 h, (d) Ti/TiC/DLC 1.0 h, (e) Ti/TiC/DLC 1.5 h and (f) Ti/TiC/DLC 2.0 h.

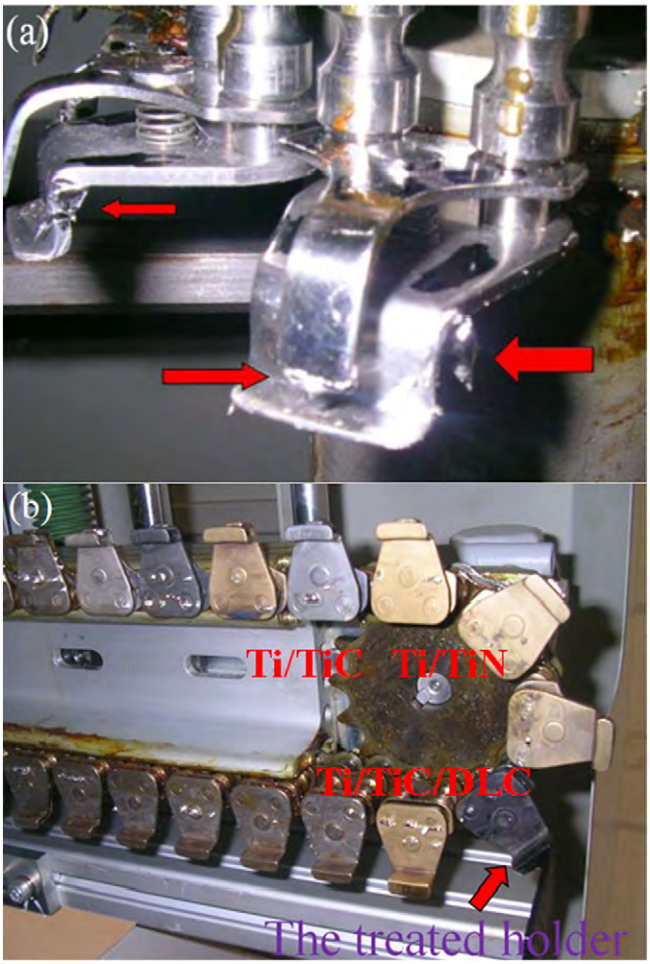

Fig. 7. Tin repellence test in wave soldering: (a) Stainless steel holders without coatings; (b) Stainless steel holders coated by Ti/TiC/DLC.

References

[1] S. Liu, S.B. Xue., J. Mater. Sci. Mater. Electron. 26 (2015) 9424.
[2] G. Chen, F. Wu, C. Liu, V.V. Silberschmidt, Y.C. Chan., J. Alloys Compd. 656 (2016) 500.
[3] A.A. El-Daly, H. El-Hosainy, T.A. Elmosalami, W.M. Desoky, J. Alloys Compd. 653 (2015) 402.
[4] T. Takemoto, M. Takemoto., Surf. MT. Tech. 18 (2006) 24.
[5] A. Forsten, H. Steen, I. Wiling, Surf. MT. Tech. 12 (2000) 29.
[6] G. Chen, F. Wu, C. Liu, V.V. Silberschmidt, Y.C. Chan, J. Alloys Compd. 656 (2016) 500.
[7] M. Jim, J. Matthew, APEX (2003).
[8] L.M. Pan, Hangzhou Electron. Technol. 2 (1991) 32.
[9] Z.L. Liu, Y.H. Guo, D.H. Chen, Eng. Plastics Appl. 41 (2003) 19.
[10] S. Xiao, Z.Z. Wu, L.L. Liu, R.K.Y. Fu, W. Li, X.B. Tian, P.K. Chu, F. Pan, Surf. Coat. Technol. (2016) online.
[11] J. Deng, M. Braun, Diam. Relat. Mater. 5 (1996) 478.
[12] J.H. Sui, W. Cai, Diam. Relat. Mater. 15 (2006) 1720.
[13] A. Shanaghi, P.K. Chu, A.R.S. Rouhaghdam, R.Z. Xu, T. Hu, Surf. Coat. Technol. 229 (2013) 151.
[14] J.H. Sui, W. Cai, Appl. Surf. Sci. 253 (2006) 2050.
[15] A. Shanaghi, P.K. Chu, R.Z. Xu, T. Hu, Vacuum 89 (2013) 238.
[16] Y.R. Xu, H.D. Liu, Y.M. Chen, M.I. Yousaf, C. Luo, Q. Wan, L.W. Hu, D.J. Fu, F. Ren, Z.G. Li, Q.S. Mei, B. Yang, Appl. Surf. Sci. 349 (2015) 93.
[17] Y.H. Wang, X. Zhang, X.Y. Wu, H.X. Zhang, X.J. Zhang, Appl. Surf. Sci. 255 (2008) 1801.
[18] M. Jelínek, K. Smetana, T. Kocourek, B. Dvoránková, J. Zemek, J. Remsa, T. Luxbacher, Mater. Sci. Eng. B 169 (2010) 89.
[19] A.C. Ferrari, J. Robertson, Phys. Rev. B 64 (2001) 075414.
[20] K.W. Chen, J.F. Lin, Thin Solid Films 517 (2009) 4916.
[21] A.A. Voevodin, M.A. Capano, S.J.P. Laube, M.S. Donley, J.S. Zabinski, Thin Solid Films 298 (1997) 107.
[22] K.L. Choy, E. Felix, Mater. Sci. Eng. A 278 (2000) 162.
[23] F. Bülbül, İ. Efeoğlu, Met. Mater. Int. 16 (2010) 573.
[24] U.H. Hwang, Thin Solid Films 254 (1995) 16.
[25] L.P. Wang, L. Huang, Y.H. Wang, Z.W. Xie, X.F. Wang, Diam. Relat. Mater. 17 (2008) 43.
[26] S.R. Polaki, N. Kumarn, K. Ganesan, K. Madapu, A. Bahuguna, M. Kamruddin, S. Dash, A.K. Tyagi, Wear 338-339 (2015) 105.
[27] W.R. Kim, M.S. Park, U.C. Jung, A.R. Kwon, Y.W. Kim, W.S. Chung, Surf. Coat. Technol. 243 (2014) 15.
[28] Z.H. Li, F.H. Meng, X.Y. Liu, Nanotechnology 22 (2011) 135302.